High Density Perforation of Thin Al-Foils with Ultra Short Pulse Lasers in Dependence on the Repetition Rate

Nelli Hambach[*1], Claudia Hartmann[*1,2], Stephan Keller[*1], Arnold Gillner[*1,2]

[*1] Fraunhofer Institute for Laser Technology, Steinbachstr. 15, 52074 Aachen, Germany
E-mail: nelli.hambach@ilt.fraunhofer.de
[*2] Chair for Laser Technology, RWTH Aachen University, Steinbachstr. 15, 52074 Aachen, Germany

Medical devices and engineering products need an increasing number of micro scaled–features, such as holes for filtration, separation and ventilation or small structures e.g. for hydrophobic effects. The size of these structures is often in the range of 20 µm and below while the structured areas grow at the same time. Therefore the factors influencing the drilling process are becoming more and more important and used to generate high process stability during the laser process. This paper investigates the process limits as well as the factors influencing the application of perforation with laser radiation of a 15 µm thick aluminum foil with UV ps-pulses. The pitch of the holes within the drilling pattern is varied as is the repetition rate used for the percussion drilling of each of the holes. The holes are evaluated by means of their diameter and shape. The precision of the hole shape is examined for two characteristics: circularity and ellipticity. Holes with a diameter of < 10 µm are drilled with pitches between 14 µm and 25 µm. Depending on the repetition rate three different drilling regimes are identified: 1. thermal drilling with increasing surface-oxidation, 2. thermal drilling with decreasing surface-oxidation and 3. shadowing of laser radiation.

DOI: 10.2961/jlmn.2016.02.0009
Keywords: laser drilling, perforation, ps-laser, thin foil drilling, stability limit

1. Introduction

Laser micro drilling and micro structuring are used for many applications such as filtration in medicine, electronics, sensor systems, medicine but also in the tooling industry [1]. For these industries to accept laser ablation, however, a fast, precise and reproducible process is still needed. The material for these filters should have a passive oxide layer to be capable for medicine and food industries. Aluminum has such an oxide layer [2].

During the last few years ps-lasers have become more and more common in industrial applications [3] [4] [5]. Thanks to their short pulse duration, the heat affected zone is reduced, but thermal effects can still occur depending on the machining parameters used [6] [7].

These thermal effects as well as other machine and process –based factors limit the stability of the laser processes. Since many products such as filters or injection molds can have very large areas that have to be drilled or structured, the laser process needs to run stably for hours or even days [2].

For the drilling of 50 µm aluminum foils with UV ns-pulses, the main factors influencing the stability of the perforation process have been identified. In this study, holes with a diameter of 20 µm or smaller were investigated. One limiting factor for the perforation process is the ellipticity of the holes. The main factors influencing the process are thermal effects in combination with the drilling strategy as well as the stability of the laser source itself [8].

When a 15 µm Al-foil is perforated with UV ps-pulses at a constant repetition rate of ν = 400 kHz, the drilling strategy has a smaller influence on the result. The minimal pitch for an in-line strategy with a hole diameter of d = 5 to 6 µm is a = 12 µm, the smallest pitch for a stable process is a = 14 µm. No further interference between the holes is observed for pitches $a \geq 19$ µm [9].

Variations of ellipticity ε and circularity γ of the drilled holes have been observed. Changes of ellipticity ε are attributed to changes in the heat distribution within the foil during the perforation process. Changes of circularity γ are attributed to either deformation of the material between the holes or to polarization [9].

The work presented here investigates the effects influencing the process stability of micro machining with ps-pulses. We studied how the repetition rate influences the drilling result and the stability limits of the percussion process for varied pitches of the holes. A 15 µm thick aluminum foil was perforated with UV ps-pulses. The perforated area was drilled in jump-and-shoot mode and each hole produced by percussion drilling. The aim is to achieve round and uniform-sized holes on large areas (containing several thousand of holes) at a large perforation degree (larger than 5%).

2. Experimental Setup

The percussion drilling experiments were carried out with a diode-pumped Nd:YVO_4 MOPA laser (Master Oscillator Power Amplifier; Hyper Rapid, LumeraLaser) with three amplification stages at a wavelength of λ = 355 nm. The laser operates at a maximum average power of P = 20 W at a repetition rate up to ν = 1 MHz and a pulse duration of τ < 15 ps. The average power can be attenuated internally. For the experiments the frequency was varied between ν = 4 kHz and 1 MHz, the pulse energy was adjusted to E = 5 µJ.

The laser beam is moved by a galvanometric scanner (intelliSCANde® 14, SCANLAB) and focused on the sample surface by a telecentric f-Θ-lens with focal length of f = 56 mm. The focus diameter is d = 10 µm. The sample material is 15 µm thick aluminum foil, which was uniformly stretched by a clamping device and positioned with linear axes. After drilling the foils were cleaned in an ultrasonic bath at 35 kHz with ethanol for 60 seconds to remove dust and debris.

Within the experiments triangular hole patterns were drilled. This serves to maximize the thermal effects, because the distance to the neighboring hole is constant in all directions. Other patterns are imaginable but may determine directed effects. Each hole pattern consists of > 3000 holes. Each hole was drilled by percussion drilling with n = 150 pulses per hole. The distance between the center of two adjacent holes is called pitch a (see Fig. 1).

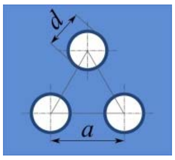

Fig. 1 Triangular hole pattern. a: pitch and d: diameter of the holes.

The variation of the pitch a leads to a change in the diameter and shape of the hole (as described before, see [9]). When the pitch is increased different regimes are observed: an instable drilling process with very small pitches, a stable drilling process for larger pitches, and drilling that has no influence between the single holes.

To investigate the influence of the repetition rate three pitches a were used:

- 14 µm: beginning of stable perforation
- 18 µm: minor influence between the holes during perforation
- 25 µm: no influence between holes during perforation.

The position and drilling order of all holes in the perforated area is defined in a coordinate list which is transferred to the scanner. As a drilling order, an "in-line" strategy was used (see Fig. 2). For this drilling strategy both the x- and the y-coordinates were arranged in ascending order.

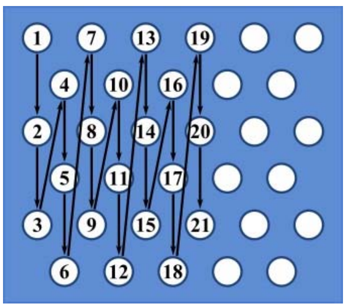

Fig. 2 The drilling order used is an "in-line" strategy.

The parameters examined in the work here presented are listed in Table 1. They were chosen according to the preliminary experiments discussed in the previous work [8] [9]. The repetition rate v and the pitch a have a very high influence on the mechanical stability of the foil. Therefore, these two parameters were varied.

The drilled holes are conical with a bigger entrance than exit diameter. For most applications the maximal transmission, meaning the maximal area removed (given as perforation degree ξ_{max}), from the foil, is of interest. Therefore, the holes are measured at the smallest dimension, the exit. The SEM pictures from exit were taken to measure the diameter. Additionally for several parameter settings, the composition of the surface elements on the side of the hole exits was analyzed by EDX to define oxide layers after the percussion process.

Table 1 Parameters used within the experiments presented in this paper.

Parameter	value
Strategy	in-line
Number of pulses	150
Pitch	14 – 25 µm
Pulse energy	5 µJ
Repetition rate	4 kHz – 1 MHz

To evaluate the drilling results, the shape of the holes was analyzed. The diameter of the holes in maximal (d_{max}) and minimal (d_{min}) dimension as well as the hole area A and the circumference U were measured from the back side (see Fig. 3).

Both dimensions are of interest as they define different aspects. For example filtration processes need a defined filtration rate at a maximal perforation degree. The filtration rate is defined by the minimal diameter of the structures as this diameter defines the largest particle size that is held back. At the same time a bigger maximal diameter enlarges the perforation rate.

To evaluate the shape of the holes, two different parameters are used: the circularity $\gamma = \frac{4\,\pi\,A}{U^2}$ and the ellipticity $\varepsilon = \frac{d_{min}}{d_{max}}$. Here, A is the measured area of the hole and U the measured circumference (see Fig. 3).

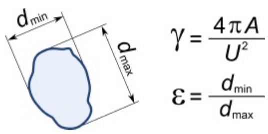

Fig. 3 Definition of circularity γ and ellipticity ε of the holes. d_{min}: minimal diameter, d_{max}: maximal diameter,
A: area of the hole and U: circumference of the hole.

When these two characteristics of the shape of the hole are defined, two different deviations from a round shape of the holes can be seen. The circularity γ changes mainly when the circumference of the hole is not smooth but does not take the overall geometry of the hole into account; however the ellipticity ε only takes the overall geometry into account and not the circumference.

The perforation degree ξ is defined as the ratio of the drilled area to the sample area. For a triangular hole pattern the perforation degree is given by:

$$\xi = \frac{A}{2\sqrt{3}\,a^2} \cdot 100\ \%$$

A is the measured hole area and a the pitch, see Fig. 1. The maximal perforation degree ξ_{max} (given by the minimal pitch) defines the maximal area which can be drilled without destroying the sample.

3. Results and Discussion

Evaluation of hole diameter:

The maximal and minimal diameters d_{max} and d_{min} in dependence of the variation of the repetition rate ν at three different pitches a = 14, 18 and 25 µm are shown in Fig. 4. The resulting diameters are between of 2 µm and 10 µm, which are relevant for e.g. filtration of tooth paste beads in wastewater [10] [11]. For both parameters, d_{min} and d_{max}, the diameter is independent of the pitch a for all investigated repetition rates ν. Both diameters d_{max} and d_{min} increase with increasing repetition rate from ν = 4 kHz to 400 kHz respectively. The main difference is the standard deviation which is much larger for the minimal diameter d_{min} than for the maximal diameter d_{max}. This larger standard deviation is caused mainly by particles which the cleaning process could not be remove (see SEM-pictures in Fig. 5). With further increasing repetition rate, the diameters d_{max} and d_{min} decrease significantly to roughly the half value from before. Additionally, the standard deviation increases dramatically for ν > 400 kHz (see Fig. 4).

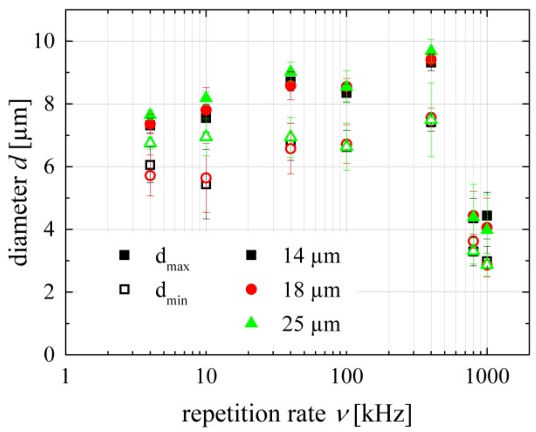

Fig. 4 Maximal and minimal diameter for variation of the repetition rate ν at three different pitches a = 14, 18 and 25 µm. (E_P = 5 µJ; n = 150)

The evaluation of the hole diameters reveals that the process for $\nu \leq$ 400 kHz is dominated by a heating effect due to increasing repetition rate. This heating effect arises because the foil material does not have not enough time to cool down after one pulse before the following pulse arrives. The time between the pulses decreases with increasing repetition rate ν. The significant decrease of the maximal diameter for ν > 400 kHz will be explained later.

Evaluation of melt:

Typical examples of the perforated areas are shown in Fig. 5, which allow a closer look at the drilling results typ. The shape of the holes is elliptical for repetition rates of $\nu \leq$ 400 kHz, the holes increasing in size with the increasing repetition rate. For larger repetition rates ν > 400 kHz the shape of the hole exit becomes triangular The behavior of the shape of the holes is nearly independent of the repetition rate ν.

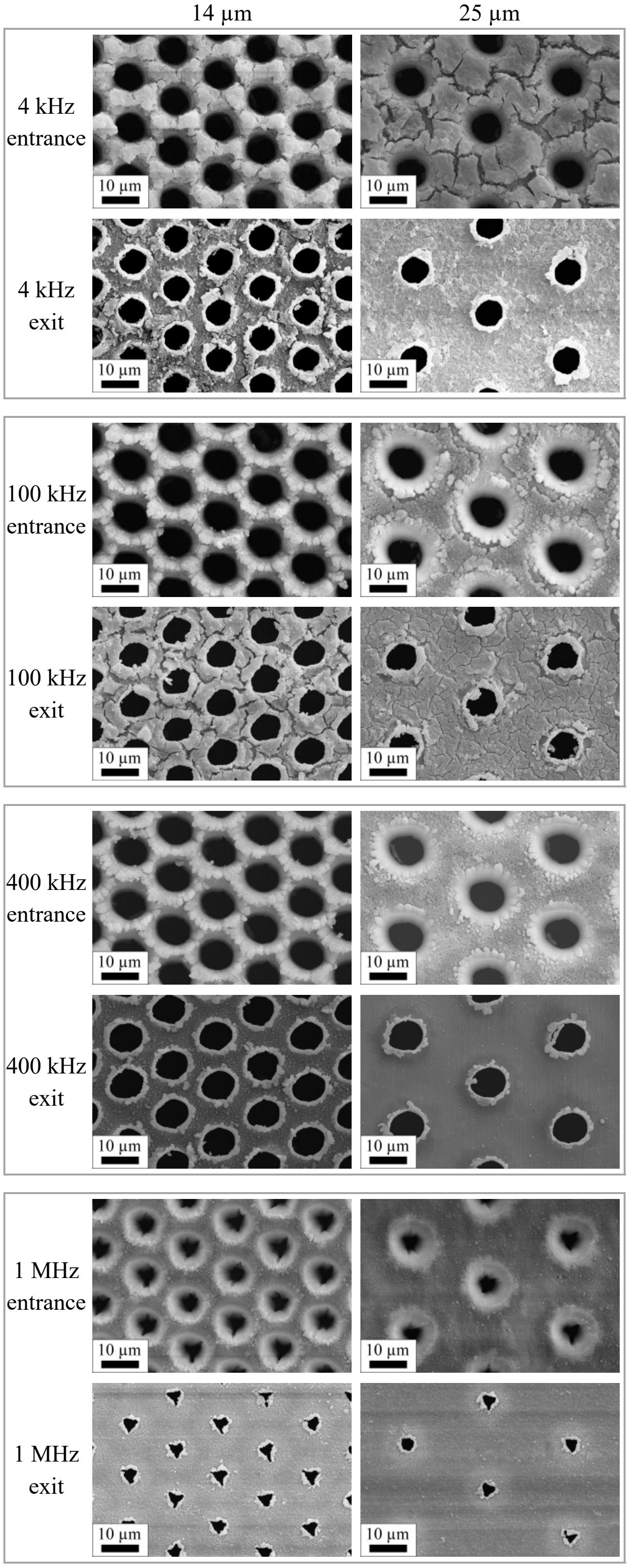

Fig. 5 SEM images of the perforated areas for the variation of the repetition rate ν at two different pitches a = 14 µm and 25 µm. (E_P = 5 µJ; n = 150)

Additionally the melting behavior changes with changing repetition rate. When drilling with $\nu = 4$ kHz on the exit side, a circular melt formation occurs. This is a solidified melt which is ejected during the perforation process. It consists of approximately 50 % aluminum (Al) and 50 % oxygen (O). The melt behavior directly around the holes is the same for all pitches a. The surface between the holes of the foil is also oxidized. For small pitches the oxidization is stronger (approximately 60 % Al, 40 % O for $a = 14$ µm) than for larger pitches (approximately 75 % Al, 25 % O for $a = 25$ µm). On the entrance side, a brittle oxide layer occurs on a large area around the holes. For larger pitches (here $a = 25$ µm, see Fig. 5), the oxide layer is smooth and cracked after the drilling process. For smaller pitches (here $a = 14$ µm) the oxide layer seems to be thicker.

When the repetition rate is increased, the melting behavior changes. When $\nu = 100$ kHz is used, a brittle oxide layer occurs on the exit side around and between the holes, (see Fig. 5). The concentration of O varies depending on the distance from the hole exit and also depending on the pitch. For $a = 14$ µm, a melt forms directly around the hole exit with a concentration of approximately 35 % O and 65 % Al. Between the holes a chemical composition of approximately 40 % O and 60 % Al is measured for all pitches a. Here the melt looks like a thin crystalline oxide layer. From these results we can conclude that two different kinds of oxides form during the drilling process. The first oxide layer (oxide directly around the holes) is a melt formation from melt expulsion during drilling. The second described oxide layer arises due to the thermal effects of the drilling process and, therefore, oxidation of the foil material. On the entrance side the melt area around the holes is much smaller than for $\nu = 4$ kHz. The melting zones have an overlap for small pitches ($a = 14$ µm, see Fig. 5).

When the repetition rate is increased further (here $\nu = 400$ kHz, see Fig. 5), a circle melt formation only arises on the exit side out of the expulsed melt with a chemical composition of approximately 45 % O and 55 % Al (similar for all pitches a). The surrounding material has only recast particles on the surface (see Fig. 5) and shows an oxygen concentration of around 20 % (for $a = 14$ µm). When the pitch a is increased the concentration of oxygen decreases to 10 to 15 % for $a = 25$ µm. This leads to the assumption that the oxidization of the surface between the holes is induced by the temperature of the foil, which increases with decreasing pitch a. From the entrance side the melt formation is similar to that of $\nu = 100$ kHz (see Fig. 5).

When the rate is increased even further, here $\nu = 1$ MHz (see Fig. 5), the sample process shows a complete different melt or oxide layer formation. On the exit side, a small melt edge occurs and very little and small debris accumulates. For all pitches a, the melt has a chemical composition of approximately 50 % Al and 50 % O. The surrounding area has a much lower oxygen concentration of maximal 10 %. The shape of the hole exit is no longer round or elliptical, but mostly triangular. On the entrance side, nearly no melt expulsion is visible and the hole shape is nearly round (see Fig. 5).

Evaluation of shape:

To characterize the holes more closely the ellipticity ε is calculated. The ellipticity ($\varepsilon = \frac{d_{min}}{d_{max}}$) takes the overall geometry of the hole into account. Fig. 6 shows the ellipticity ε for the three different pitches $a = 14$, 18 and 25 µm depending on the repetition rate ν.

First, the ellipticity ε decreases with increasing repetition rate for $\nu \leq 10$ kHz (regime I). When the repetition rate is increased further $\nu \leq 400$ kHz, the ellipticity ε increases slightly or remains constant (regime II). For $\nu > 400$ kHz the ellipticity ε decreases significantly (regime III).

The circularity $\gamma = \frac{4\pi A}{U^2}$ is used to evaluate how smooth the circumference of the hole is. The circularity γ for the three different pitches $a = 14$, 18 and 25 µm, each depending on the repetition rate ν, is shown inFig. 7.

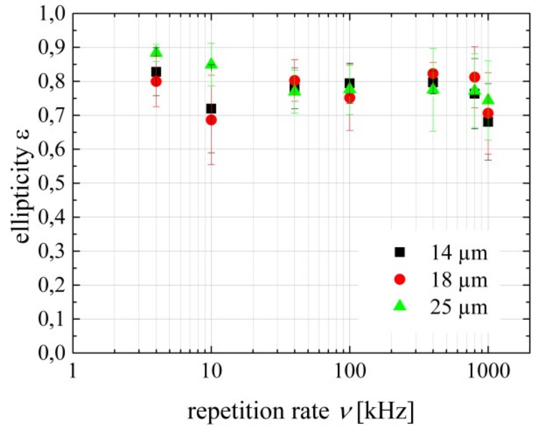

Fig. 6 Ellipticity ε depending on the repetition rate ν at three different pitches $a = 14$, 18 and 25 µm. ($E_P = 5$ µJ; n = 150)

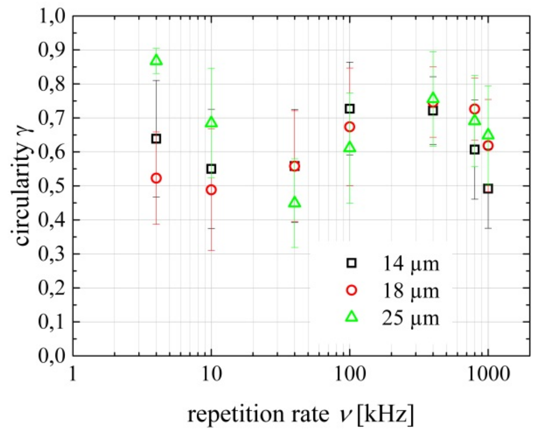

Fig. 7 Circularity γ depending on the repetition rate ν at three different pitches $a = 14$, 18 and 25 µm. ($E_P = 5$ µJ; n = 150)

When the circularity γ is similar to the ellipticity ε, the same three different regimes are found. The standard deviation of the circularity γ is much larger that of the ellipticity ε. The influence of particles which could not be removed by the cleaning process depends much more on the circularity γ than on the ellipticity ε.

Three different regimes can be identified:

- Regime I:
  for $\nu \leq 10$ kHz resp. $\nu \leq 40$ kHz for $a = 25$ µm
- Regime II:
  for 10 kHz < $\nu \leq 400$ kHz resp. for 40 kHz < $\nu \leq$ 400 kHz for $a = 25$ µm
- Regime III:
  for $\nu > 400$ kHz

Evaluation of perforation degree:

For several applications the perforation degree $\xi = \frac{A}{2\sqrt{3}\,a^2} \cdot 100\,\%$ is of interest [11]. Fig. 8 shows the perforation degree ξ for the variation of the repetition rate ν at the three investigated pitches $a = 14$, 18 and 25 µm .

The perforation degree ξ grows with increasing repetition rate ν until it reaches a maximum at $\nu = 400$ kHz. A further increase of the repetition rate ν leads to a significant decrease of the perforation degree ξ for all investigated pitches a. This indicates a different ablation behavior for $\nu \leq 400$ kHz and $\nu > 400$ kHz.

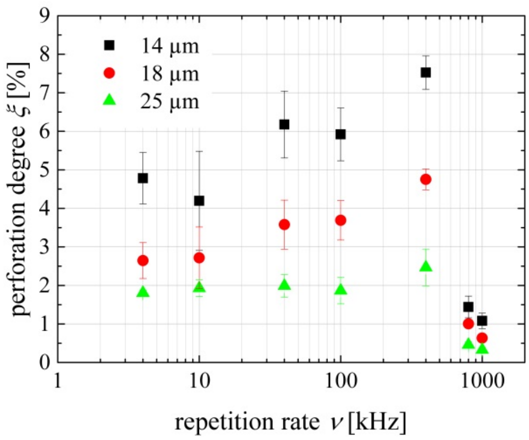

Fig. 8 Perforation degree ξ for the variation of the repetition rate ν at three different pitches $a = 14$, 18 and 25 µm. ($E_P = 5$ µJ; n = 150)

The variation in the pitch a also leads to a change in the behavior of the perforation degree ξ. A pitch of $a = 25$ µm causes an increase in the perforation degree ξ of 30 % for repetition rates $\nu \leq 400$ kHz, while pitches $a \leq 18$ µm cause an increase in the perforation degree ξ of 80 % for repetition rates $\nu \leq 400$ kHz.

This leads to the conclusion that for the pitch of $a = 25$ µm the holes influence each other only very little during the perforation process since a lack of heat dissipation between the holes causes a thermal heat blocking within the drilled foil. For smaller pitches, $a \leq 18$ µm, the heat cannot dissipate due to the little remaining material between the drilled holes. Therefore, the perforation process is heat dominated and leads to deformation effects as discussed previously [9].

The maximal perforation degree achieved within the experiments is $\xi_{max} = 7.5$ %. This is a perforation degree typically required by filter applications [11].

Resulting drilling regimes:

The drilling behavior described before can be identified with respect to diameter d_{min}, d_{max}, ellipticity ε, circularity γ and melting respectively oxidization behavior of three different regimes for different repetition rates ν.

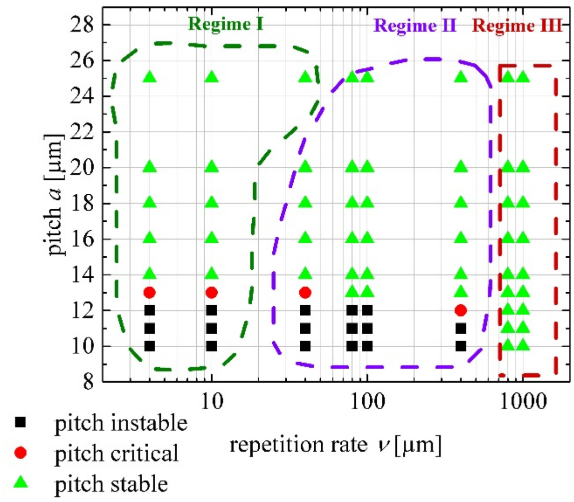

Fig. 9 Stability of drilled foil with different pitches a for the variation of the repetition rate ν. Regime I green line, regime II violet line, regime III red line ($E_P = 5$ µJ; n = 150)

- **Regime I**: thermal drilling with increasing surface oxidation (Fig. 9 dark green dashed line)
  - for $a < 25$ µm: $\nu \leq 10$ kHz
  - for $a = 25$ µm: $\nu \leq 40$ kHz

  The drilling behavior shows a thermal influence. Since the repetition rate increases the heat cannot be dissipated fast enough within the foil before the next pulse arises. The foil heats up during drilling. This results in increasing hole diameters d_{min} and d_{max}.
  Within this regime with increasing repetition rate ν more debris or melt droplets remain in the holes and cannot be removed. This leads to a decrease of ellipticity ε and circularity γ.
  Since the foil is heated increasingly the material between the holes oxidizes analogous to its heating and a stable oxide layer is generated.
- **Regime II**: thermal drilling with decreasing surface oxidation (Fig 9 violet dashed line)
  - for $a < 25$ µm: 10 kHz < $\nu \leq 400$ kHz
  - for $a = 25$ µm: 40 kHz < $\nu \leq$ 400 kHz

  The thermal build up accumulation due to repetition rate ν increases further. The heat cannot be dissipated fast enough within the foil before the next pulse arises. The foil heats up even more during drilling. This results in hole diameters d_{min} and d_{max} increasing further.
  The drilling process is stable, and the ellipticity ε remains nearly constant within this regime. The circularity γ, mostly depending on remaining melt droplets in the drilled holes, increases with increasing repetition rate ν. This indicates that the

melt removal has improve and is more homogeneous.
The surface of the material between the holes still oxidizes due to thermal heating, but the concentration of oxygen within the oxide layer decreases. This could be caused by different kinds of oxidation due to different surface temperatures and surface conditions caused by a change of drilling parameters. This has to be evaluated in future.
At the end of regime II the diameters are largest of all parameters therefore here the largest maximal perforation degree ξ_{max} can be achieved.

- **Regime III**: shadowing of laser radiation (Fig. 9 red dashed line)
  - for all pitches a: $\nu > 400$ kHz

  In this regime the laser radiation is shadowed which means it is both, blocked and scattered by the metallic dust generated during drilling. This dust remains in the surroundings of the holes and cannot be spread fast enough due to the high repetition rate of the laser. There is a critical repetition rate ν_{crit} when the dust becomes optically thick and therefore starts to impair the drilling process. ν_{crit} has to be defined exactly in future.
  Due to the shadowing of the laser radiation the drilling process becomes inhomogeneous. Therefore this shadowing effect has an influence not only on the hole diameter d_{min} and d_{max}, but also the hole shape, which is mostly triangular.
  Within this regime only little melt remains on the surface of the entrance side. From the exit side a small melt edge forms with very little and small debris. This melt edge has a composition of 50 % aluminum and 50 % oxygen. The surrounding foil of the holes is only oxidized a little and has a maximum of 10 % oxygen.

For a better overview the stability of the drilling process is shown in Fig. 9. The black colored squares show the instable pitch. This means the foil is molten between two holes, or whole areas are broken out. The green triangles stand for the stable pitch. This means no cracks appear and the foil is mechanically stable. The red dots stand for the process within the critical sector. Foils drilled with this pitch have cracks or the melt formation on the top of the foil is covering the neighbor holes too much.

4. Conclusion and outlook

Stable processes are important for micro drilling and structuring as the areas to be machined get bigger and bigger. The laser processes have to be stable for hours or even days. Therefore, the factors influencing the stability of micro machining with ps-pulses have to be determined.

In the work described here the drilling behavior in dependence on the repetition rate ν was analyzed for different pitches a of the holes. This is done for percussion drilling of large areas with a UV ps-laser. To analyze the drilling behavior the holes are measured with respect to diameter d_{min}, d_{max}, ellipticity ε and circularity γ. Additionally the oxidation of the foil on the exit side is evaluated.

Depending on the repetition rate ν, three different drilling regimes are defined:

Regime I: thermal drilling with increasing surface oxidation. ($\nu \leq 10$ kHz and 40 kHz for $a < 25$ µm and 25 µm, respectively) The drilling behavior is thermally influenced and the diameter of the holes increases whereas ellipticity and circularity decrease. The foil material between the holes oxidizes analogous to the heating effect.

Regime II: thermal drilling with decreasing surface oxidation. (10 kHz and 40 kHz $< \nu \leq 400$ kHz for $a < 25$ µm and $a = 25$ µm, respectively). The thermal influence increases further and results in further increasing hole diameter. The melt removal improves, which leads to increasing ellipticity and circularity. The concentration of oxygen within the oxide layer on the surface between the holes decreases. This could be caused by different kinds of oxidation due to different surface temperatures and surface conditions and has to be evaluated in the future. In this regime the largest maximal perforation degree was achieved.

Regime III: shadowing of laser radiation. ($\nu > 400$ kHz) The laser radiation is blocked and scattered by the metallic dust generated during drilling. The shadowing effect causes an inhomogeneous drilling result with small, mostly triangular holes. The foil between holes is nearly not oxidized.

These results indicate that the thermal coefficient of the foil material has a large influence on the drilling results. Further investigations will be done with other materials with larger and/or lower thermal coefficient in order to prove this thesis.

Acknowledgments and Appendixes
Parts of the research depicted here were funded by the German Research Foundation DFG as part of the Cluster of Excellence "Integrative Production Technology for High-Wage Countries”.

References

[1] J. Bekesi, J.J.J. Kaakkunen, W. Michaeli, F. Klaiber, M. Schoengart, J. Ihlemann, and P. Simon: Appl. Phys., A99, (2010) 691.
[2] I. Gehrke: „Metallische Mikrosiebe“ (Logos Verlag, Berlin, 2008) p. 4-11.
[3] R. Knappe and A. Nebel: Proc. of SPIE, 6871, (2008) 687121.
[4] A. Gillner, A. Dohrn and C. Hartmann: 3rd International CIRP High Performance Cutting Conference, (2008) 199
[5] G. Rutterford, D. Karnakis, A. Webb and M. Knowles: Proc. ALAC, (2005)
[6] S. Bruening, G. Hennig, S. Eifel and A. Gillner: Phys. Proc., 12, (2011) 105
[7] A. Luft, U. Franz, A. Emsermann and J. Kaspar: Appl. Phys., A63, (1996) 93.
[8] N. Hambach, C. Hartmann, J. Holtkamp and A. Gillner: J.of Laser Appl., 24, (2012) 032001.
[9] Hartmann, C., Hambach, N., Jüngst, M., Keller, S., Holtkamp, J., and Gillner: A. J. Laser Micro/Nanoeng., 8, (2013) 266–270.

[10] http://www.protecingredia.com/index.html

[11] "Microfluidics: Technologies and Global Markets", BCC Research, 2013

(Received: May 26, 2015, Accepted: April 25, 2016)